Observation of quantum confinement in the occupied states of diamond clusters

T. M. Willey,[1,*] C. Bostedt,[2] T. van Buuren,[1] J. E. Dahl,[3] S. G. Liu,[3] R. M. K. Carlson,[3] R. W. Meulenberg,[1] E. J. Nelson,[1] and L. J. Terminello[1]

[1]*Lawrence Livermore National Laboratory, Livermore, California 94550, USA*

[2]*Technische Universität Berlin, PN 3-1, Hardenbergstrasse 36, 10623 Berlin, Germany*

[3]*MolecularDiamond Technologies, Chevron, P. O. Box 1627, Richmond, California 94802, USA*

(Received 31 August 2006; published 28 November 2006)

Condensed-phase hydrogen-terminated diamond clusters (diamondoids) have been studied with soft-x-ray emission and x-ray-absorption spectroscopy. The occupied and unoccupied electronic states measured with these methods imply an increasing highest occupied molecular orbital–lowest unoccupied molecular orbital gap with decreasing diamondoid size, with the shifting entirely in the occupied states, in contrast to other semiconductor nanocrystals. These experimental results are compared with theoretical calculations on the electronic structure of diamondoids.

DOI: 10.1103/PhysRevB.74.205432 PACS number(s): 36.40.−c, 73.22.−f, 81.07.Nb

I. INTRODUCTION

The availability of hydrogen-terminated diamondlike clusters, or diamondoids,[1] opens a wealth of possibilities in nanoscience and technology. These clusters bridge the gap between diamond nanocrystals and small hydrocarbon molecules. Diamondoids enable the experimental study of the evolution of the electronic structure in sp^3 carbon from the bulk to the molecular limit, and allow experimental studies of quantum confinement in a size-selected and perfectly hydrogen terminated series of carbon clusters.

Diamond nanocrystals have different properties than other group IV semiconductors such as silicon and germanium. Si and Ge nanocrystals exhibit quantum confinement, with decreasing sizes leading to increasing band gap through evolution in both the conduction and valence bands.[2,3] X-ray absorption shows that diamondoids exhibit negligible shifting in the lowest unoccupied states, and these states are dominated by the hydrogen surface termination that must be considered an integral part of the electronic structure.[4] Although initial calculations indicated shifting in these lowest unoccupied molecular orbitals,[5] the experimental evidence is supported by the most recent calculations showing that if quantum confinement effects exist in diamond, the changes will occur predominantly in the highest occupied states.[6,7] Further, unlike Si and Ge, diamond is predicted to have size effects on electronic structure only below 1 nm.[5,8,9]

Even though calculations on these small molecules would appear straightforward, recent theoretical calculations of highest occupied molecular orbital–lowest unoccupied molecular orbital (HOMO-LUMO) gaps in diamondoids show large variation. For example, the calculated gap value for adamantane ranges from 9.3 eV (Ref. 7) to 5.77 eV.[6] Perhaps even more controversial is the discrepancy in the relative change in gap calculated through the diamondoid series. Density-functional theory (DFT) calculations predict that adamantane has a gap about 1 eV (Refs. 5 and 7) or 0.74 eV (Ref. 6) larger than pentamantane, while quantum Monte Carlo (QMC) methods predict a difference of about 0.57 eV.[6] Thus, experimental measurement of the occupied states of diamondoids is an imperative step toward understanding the evolution of electronic structure and resolving conflicting calculational predictions of quantum confinement in diamond.

In this paper, we measure the filled and empty electronic states of the diamondoid series presented in Fig. 1. These measurements, as opposed to previous gas-phase work,[4] are performed on technologically relevant condensed-phase diamondoids.[10] X-ray-absorption spectroscopy (XAS) from the carbon 1*s* level probes the unoccupied states and indicates the relative energy position of the lowest unoccupied orbitals.

Soft-x-ray emission (SXE) spectroscopy aptly probes the highest occupied sp^3 hybridized states in diamondoids.[11,12] Although photoemission achieves higher resolution and signal to noise, the highly insulating nature of diamondoid powders produces energy broadening and shifting of photoemission features, obscuring reproducible determinations of shifts between different diamondoid samples. In contrast, the photon-in/photon-out nature of the x-ray emission spectroscopy effectively mitigates these difficulties, with reproducible energy scales for different diamondoid powders. In this work, the changes seen in the soft-x-ray emission as a function of diamondoid size are presented.

These two techniques (XAS and SXE) provide independent measures of the unoccupied and occupied states, and

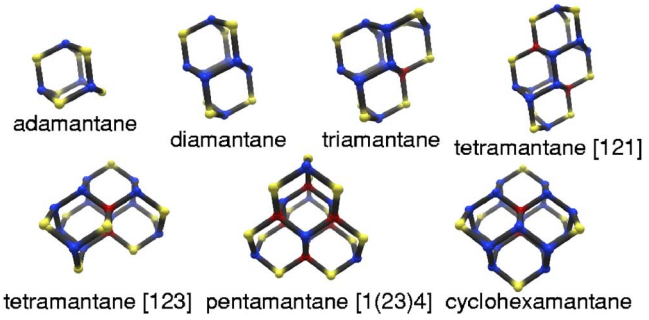

FIG. 1. (Color online) Diamondoids investigated from adamantane to cyclohexamantane viewed along the diamond bulk lattice [110] vector. Colors indicate bulk-coordinated, CH, and CH_2 with red, blue, and yellow, respectively.

give an indication of the LUMO and HOMO relative energies. From these data, the gaps of the diamondoids are estimated and compared to the various calculations.

II. EXPERIMENTAL

The diamondoids are extracted from petroleum and size and shape separated by high-performance liquid chromatography producing ultrahigh purity molecules.[1] Figure 1 shows structures of the investigated diamondoids adamantane, diamantane, triamantane, [121] tetramantane, [123] tetramantane, [1(2,3)4] pentamantane, and cyclohexamantane.[13] The size-selected diamondoids range in diameter from about 0.5 nm to about 1 nm, and are fully sp^3 hybridized, exhibiting a complete hydrogen surface termination. Adamantane and diamantane consist of carbon surface atoms, while triamantane exhibits the first fully bulk-coordinated carbon atom. Tetramantane has three isomers (one with two enantiomers), while larger diamondoids have both multiple isomers and weight classes. This multiplicity is demonstrated in the range of calculated gap values from the literature for a given polymantane order presented later. Here, we investigate the compact tetrahedral [1(2,3)4] pentamantane, with a high fraction of bulk-coordinated atoms, and cyclohexamantane.

For these measurements, solid diamondoid powders were pressed into clean indium foil. The lower diamondoids (adamantane-triamantane) sublime readily in vacuum at room temperature; thus all diamondoids were cooled in vacuum to within a few degrees of liquid nitrogen before data acquisition. Data were acquired at a background pressure in the analysis chamber of 10^{-8} torr, with a high partial pressure of the subliming diamondoids.

The soft-x-ray emission (a probe of the filled states[14]) and x-ray absorption spectra (a probe of the empty states[15]) were collected at undulator beamline 8.0 of the Advanced Light Source at Lawrence Berkeley National Laboratory.[16] The fluorescence endstation utilizes a Rowland circle grating emission spectrometer with an area detector. The spectrometer is fixed at 90 degrees from the incident x rays. The powder samples were oriented at 45 degrees from the incident radiation and fluorescence spectrometer. The resolution of the spectrometer was set to be about 0.5 eV based on the full width at half-maximum (FWHM) of the elastic peak; this was a good balance between resolution, count rate, and x-ray dose on the diamondoids. This instrumental broadening, however, does not limit determination of the positions of features within the spectra. The XAS measurements used total electron yield (TEY), with an upstream clean gold grid for normalization.[15] The photon flux was adjusted to minimize photochemical changes in XAS spectra, and required measurements over multiple experimental runs. Highly oriented pyrolytic graphite (HOPG) C *K*-edge absorption was measured to calibrate the photon energy output of the beamline monochromator. Elastically scattered photons, appearing in the emission spectral window when tuned near the absorption onset, were used to calibrate the fluorescence energy scales.

III. RESULTS

Figure 2 shows the soft-x-ray emission and the x-ray-absorption spectra for the diamondoid series. The XAS spectra are similar in shape to gas-phase absorption spectra,[4] but lack the vibronic fine structure in the features in the lowest energy states at 287–289 eV. These features are below the bulk absorption onset, and are similar in energy to hydrogen-terminated diamond surface states.[17,18] Note that through the diamondoid series, the absorption onset, within experimental error (~0.05 eV over multiple experimental runs) does not change. These data confirm the earlier results[4] that show the lowest unoccupied states are dominated by the hydrogen surface termination and quantum confinement does not appreciably affect the LUMO in diamondoids.

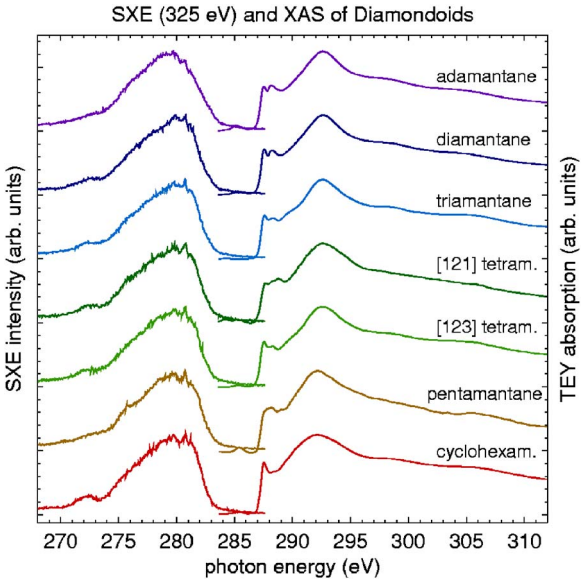

FIG. 2. (Color online) Soft-x-ray emission spectra acquired with excitation energy 325 eV on the left; x-ray absorption of the diamondoid series on the right.

The fluorescence emission spectra are presented on the left side of Fig. 2. All diamondoid emission spectra exhibit a similar shape. The feature at about 272 eV is related to states with 2*s* character[12] while the more intense fluorescent features closer to the highest occupied orbitals arise from states with 2*p* character. The fluorescent photons, emitted as valence states decay into the C 1*s* core hole, map the energy of the highest occupied states.

The inflection position of the soft-x-ray emission indicates the change in energy of the highest occupied states in this series of diamondoids. This method was chosen because hydrocarbons can be unstable under intense x rays required to produce sufficient carbon fluorescence.[19] Figure 3 shows one example of diamantane continuously moved in the x-ray beam during acquisition (solid line) versus a SXE spectrum acquired continuously for 300 s on the same area of sample.[20] Under soft x rays, intensity gradually appears at about 282 eV as indicated by the arrow. This intensity can be attributed to sample damage under x-ray illumination. Also, the 2*s* state is no longer clearly resolvable. Thus, all SXE spectra were acquired while rastering the sample in the x-ray beam. The intersection of the linear extrapolation of the edge to the baseline has been used as an indication of the top of the valence band in previous publications on quantum con-

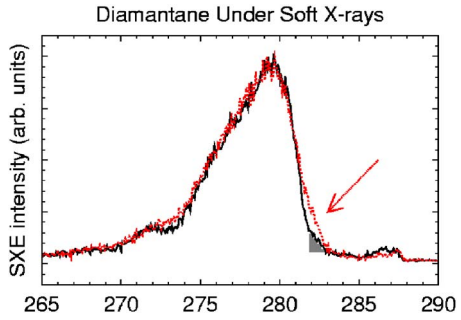

FIG. 3. (Color online) Diamantane with minimal photochemical changes (black, solid) and under the beam continuously for 300 s (red, dotted line) showing spurious intensity (arrow) appearing near the HOMO states.

finement effects in semiconductor nanocrystals.[2] However, even the initial stages of x-ray beam damage can obscure the intersection of the SXE with the background (gray shaded area). To avoid uncertainties related to beam damage effects, the inflection point of the valence-band edge is chosen as a basis for the discussion of size-dependent changes in the electronic structure as it is a more precise measure of the change in energy of the highest occupied states.

The inflection positions were found by finding the minima of the derivatives of the SXE spectra. Derivatives were obtained by calculating the slopes at each point of SXE curves via linear regression using four, six, and eight points (0.25, 0.37, and 0.5 eV respectively) on each side of the point of interest. A subset of these derivatives is shown in the lower pane of Fig. 4, with the minima in each case also indicated. The inflection positions and respective lines are superimposed on the SXE data in the top pane of Fig. 4. The inflections clearly evolve and shift toward lower energy with decreasing size through the diamondoid series relative to the constant excitation energy, seen as the elastic line at 287.8 eV in this figure.

To obtain the relative energy shift of the highest occupied states in the diamondoid series from adamantane to hexamantane, and to probe SXE intermediate state effects,[14] the incident excitation energy was varied from the lowest unoccupied surface features associated with the hydrogen surface termination (287.6, 287.8, and 288.1 eV) to the carbon-carbon σ^* (292.2 eV) to well above the C 1*s* photoabsorption threshold (325.2 eV).[20] Figure 5 shows the inflection point energy positions of the diamondoid soft-x-ray emission spectra consistently move toward lower energy with decreasing size; the relative shift between adamantane and pentamantane is 0.6+/−0.2 eV. Although the spectra do not exhibit prominent energy-dependent resonant inelastic scattering (RIXS) features as in bulk diamond,[21] with excitations into LUMO-like states, the emission at the highest occupied states is consistently lower in energy by 0.3+/−0.1 eV. These excitation energy-dependent phenomena may be due to different intermediate states or inequivalent carbon sites. The soft x-ray emission acquired at each and every excitation energy (i.e., each pane of Fig. 5) exhibits an energy shift correlated to diamondoid size. Thus, irrespective of the intermediate state, the soft x-ray emission and thus the highest

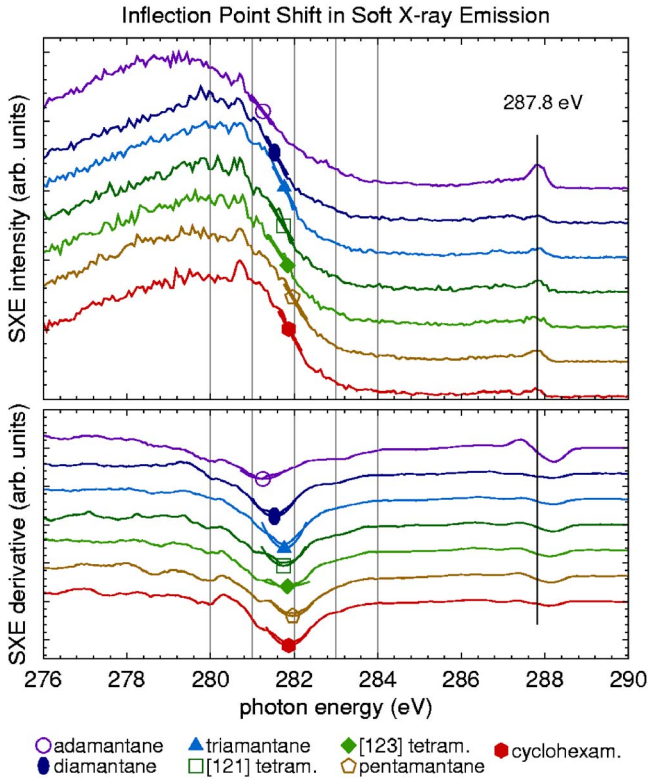

FIG. 4. (Color online) Top: SXE spectra, showing the inflection point and a line fit through the data near the inflection point. Bottom: The smoothed derivatives of the SXE spectra, with the minima (the inflection point) indicated. The excitation elastic line is visible at 287.8 eV.

occupied states are shifting to lower energy with decreasing size, measured to the indicated precision. These experimental errors are the extrema of minima from multiple derivatives derived from each spectrum coupled with the uncertainty in the calibration of the energy scales of the fluorescence spectrometer through fitting of the elastic peak. In general, confidence levels lie within +/−0.1 eV with the exception of adamantane. This diamondoid sublimed rapidly (vapor pressure at 300 K is $\sim 10^{-4}$ torr) and left much smaller areas for analysis. Thus, adamantane samples required slower rastering that led to larger beam-damage features in the spectra from this particular diamondoid. These issues are reflected in the greater uncertainty in the adamantane measurements.

HOMO-LUMO gaps were estimated by comparing the diamondoid inflection points of the SXE and XAS and comparing these to the respective inflection points in the concurrently acquired bulk diamond spectra.[9,21–23] The energy differences were systematically adjusted such that bulk-diamond edges (SXE excitation energy at 325 eV) yielded the well-known experimental gap of 5.47 eV.[24] Small differences between diamond and diamondoid core-hole effects in the x-ray absorption,[25] and the presence of the core exciton in the bulk diamond absorption,[26] will affect the relative position of the diamond versus diamondoid unoccupied states.[23] These differences between bulk diamond and diamondoids are expected to affect the absolute estimation of the gaps. However, the measured LUMO energy is constant

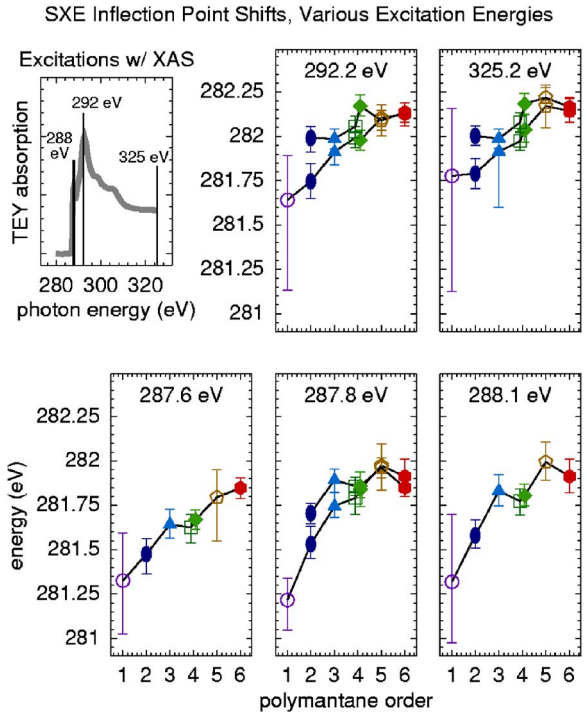

FIG. 5. (Color online) Trends observed in the inflection point of the high-energy side of the SXE spectra, using various excitation energies.

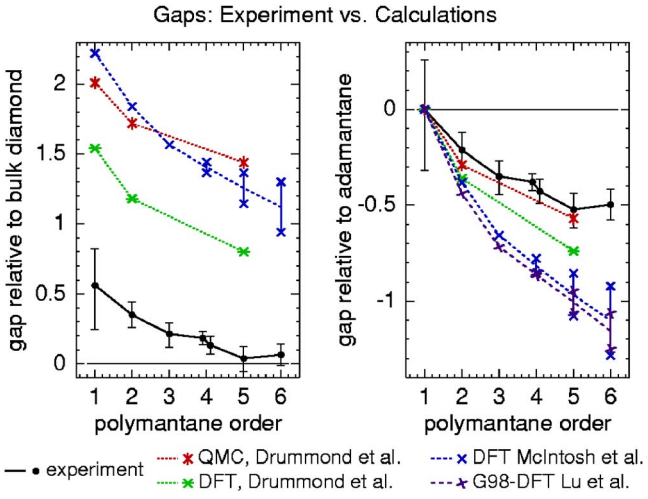

FIG. 6. (Color online) Comparison of the gap inferred from experiment to calculations on diamondoids thus far in the literature. At left, gaps are plotted vs the bulk value obtained using the same method used to derive the corresponding diamondoid gaps. At right, the relative shifts are compared by plotting the gaps relative to adamantane. Calculations are QMC and DFT by Drummond *et al.* (Ref. 6) DFT by McIntosh *et al.* (Ref. 5), and GAUSSIAN 98 DFT by Lu *et al.* (Ref. 7).

across the diamondoid series to less than 0.05 eV, and these issues will not affect the measured precision of the occupied states. The core-hole effects in analogous systems do not appreciably shift the soft x-ray emission[23,25] and the SXE profiles are similar for all of the diamondoids, so the relative change in the energy position of the occupied states can be measured with the precision indicated in Fig. 5. The average of all of the data in Fig. 5 with appropriate error propagation,[27] in conjunction with XAS as a probe of the LUMO (Fig. 2), leads to the estimated gaps listed as a part of Table I.

IV. DISCUSSION

The changing energy positions of the occupied states lead to an experimentally derived gap that is very similar in pentamantane (possesses most bulk-coordinated atoms in this series) and bulk diamond, and increases with decreasing size by ~0.5 eV at adamantane. The absolute estimate of the gaps is roughly consistent with the absolute calculated values that are both larger and smaller than the experimental estimate, as seen in Table I. More importantly, Fig. 6 shows the experimentally derived gap values compared to the diamond bulk band-gap value (left pane) and the relative change across the series by plotting gap values relative to adamantane (right pane). As seen in the left pane of Fig. 6, the models, when plotted relative to the bulk value calculated in the same fashion (see Table I), all overestimate the experimentally derived values for diamondoids. In this case, the closest model to the data is DFT calculations where the basis sets were chosen to more properly represent the extended LUMO and the associated surface states.[6] This treatment is still not sufficient to match the experimental data, but note calculations are on noninteracting clusters, while measurements use condensed-phase diamondoids, and particle-particle interaction may play a role.[10] The experimental gap is also affected by the core hole and core exciton in x-ray absorption. These issues are not considered in the calculations, and could account for a portion of the 1 eV absolute discrepancy between experiment and the closest model. On the other hand, the measured fixed-energy absorption onset and variable-energy inflection provide a precise measure of the change in gap from one diamondoid to the next. Thus, in perhaps the most interesting comparison, the right pane in Fig. 6 illustrates the relative change in gaps through the diamondoid series. The quantum Monte Carlo simulations provide the best fit between experiment and theory, and appear to be the most accurate in predicting the relative change in gap. DFT calculations, compared to this dataset, overestimate the relative change in gap. Among the DFT calcula-

TABLE I. HOMO-LUMO gaps estimated from the SXE data, along with recent calculations from the literature.[5–7]

	SXE-XAS	DFT[a]	DFT[b]	QMC[b]	G98[c]
adamantane	6.03	7.62	5.77	7.61	9.33
diamantane	5.82	7.24	5.41	7.32	8.89
triamantane	5.68	6.97			8.61
tetramantanes	5.60–5.65	6.77–6.84			8.46–8.47
pentamantanes	5.51	6.54–6.77	5.03	7.04	8.26–8.38
hexamantanes	5.54	6.34–6.70			8.07–8.26
bulk diamond	5.47	5.4	4.23	5.6	

[a]Reference 5.
[b]Reference 6.
[c]Reference 7.

tions, careful treatment of the diffuse character of the surfaces states predicts a less drastic change in the gap across the series, leading to a better fit with the data.

V. CONCLUSIONS

In summary, soft-x-ray emission and x-ray absorption adamantane, diamantane, triamantane, [121] tetramantane, [123] tetramantane, [1(2,3)4] pentamantane, and cyclohexamantane have been measured. The inflection points on the high-energy side of emission spectra, an indication of energy positions of the highest occupied states, shifts toward lower energy in the diamondoids with decreasing size. Solid-state diamondoid x-ray absorption also indicates, as reported previously in the gas phase, that the lowest unoccupied states are relatively fixed in energy and dominated by states associated with the hydrogen-terminated surface. These results imply an increasing HOMO-LUMO gap with decreasing size, where energy shifting, and by extension quantum confinement, occurs only in the occupied states.

ACKNOWLEDGMENTS

This work was performed under the auspices of the U.S. DOE by LLNL under Contract No. W-7405-ENG-48. The Advanced Light Source is supported by the U.S. DOE, Contract No. DE-AC02-05CH11231. Additional supporting experiments were performed at The Stanford Synchrotron Radiation Laboratory, supported by the U.S. DOE, Basic Energy Sciences.

*Email address: willey1@llnl.gov

[1] J E. Dahl, S G. Liu, and R. M. K. Carlson, Science **299**, 96 (2003).
[2] T. van Buuren, L. N. Dinh, L. L. Chase, W. J. Siekhaus, and L. J. Terminello, Phys. Rev. Lett. **80**, 3803 (1998).
[3] C. Bostedt, T. van Buuren, T. M. Willey, N. Franco, L. J. Terminello, C. Heske, and T. Möller, Appl. Phys. Lett. **84**, 4056 (2004).
[4] T. M. Willey, C. Bostedt, T. van Buuren, J. E. Dahl, S. G. Liu, R. M. K. Carlson, L. J. Terminello, and T. Möller, Phys. Rev. Lett. **95**, 113401 (2005).
[5] G. C. McIntosh, M. Yoon, S. Berber, and D. Tománek, Phys. Rev. B **70**, 045401 (2004).
[6] N. D. Drummond, A. J. Williamson, R. J. Needs, and G. Galli, Phys. Rev. Lett. **95**, 096801 (2005).
[7] A. J. Lu, B. C. Pan, and J. G. Han, Phys. Rev. B **72**, 035447 (2005).
[8] D. A. Areshkin, O. A. Shenderova, S. P. Adiga, and D. W. Brenner, Diamond Relat. Mater. **13**, 1826 (2004).
[9] J.-Y. Raty, G. Galli, C. Bostedt, T. W. van Buuren, and L. J. Terminello, Phys. Rev. Lett. **90**, 037401 (2003).
[10] C. Bostedt, T. van Buuren, T. M. Willey, and L. J. Terminello, Appl. Phys. Lett. **85**, 5334 (2004).
[11] K. Endo, S. Koizumi, T. Otsuka, M. Suhara, T. Morohasi, E. S. Kurmaev, and D. P. Chong, J. Comput. Chem. **22**, 102 (2001).
[12] K. Endo, S. Koizumi, T. Otsuka, T. Ida, T. Morohashi, J. Onoe, A. Nakao, E. Z. Kurmaev, A. Moewes, and D. P. Chong, J. Phys. Chem. A **107**, 9403 (2003).
[13] A. T. Balaban and P. R. von Schleyer, Tetrahedron **34**, 3599 (1978).
[14] A. Kotani and S. Shin, Rev. Mod. Phys. **73**, 203 (2001).
[15] J. Stöhr, *NEXAFS Spectroscopy*, Springer Series in Surface Sciences (Springer-Verlag, Berlin, 1992).
[16] J. J. Jia *et al.*, Rev. Sci. Instrum. **66**, 1394 (1995).
[17] R. Graupner, J. Ristein, L. Ley, and C. Jung, Phys. Rev. B **60**, 17023 (1999).
[18] A. Hoffman, G. Comtet, L. Hellner, G. Dujardin, and M. Petravic, Appl. Phys. Lett. **73**, 1152 (1998).
[19] M. Zharnikov and M. Grunze, J. Vac. Sci. Technol. B **20**, 1793 (2002).
[20] See EPAPS Document No. E-PRBMDO-74-034644 for the relevant and complete set of soft x-ray emission spectra. For more information on EPAPS, see http://www.aip.org/pubservs/epaps.html
[21] Y. Ma, N. Wassdahl, P. Skytt, J. Guo, J. Nordgren, P. D. Johnson, J. E. Rubensson, T. Boske, W. Eberhardt, and S. D. Kevan, Phys. Rev. Lett. **69**, 2598 (1992).
[22] Y. Ma, P. Skytt, N. Wassdahl, P. Glans, D. C. Mancini, J. Guo, and J. Nordgren, Phys. Rev. Lett. **71**, 3725 (1993).
[23] E. L. Shirley, J. Electron Spectrosc. Relat. Phenom. **110**, 305 (2000).
[24] C. D. Clark, P. J. Dean, and P. V. Harris, Proc. R. Soc. London, Ser. A **277**, 312 (1964).
[25] E. L. Shirley, Phys. Rev. Lett. **80**, 794 (1998).
[26] J. F. Morar, F. J. Himpsel, G. Hollinger, G. Hughes, and J. L. Jordan, Phys. Rev. Lett. **54**, 1960 (1985).
[27] J. R. Taylor, *An Introduction to Error Analysis: The Study of Uncertainties in Physical Measurements* (University Science Books, Mill Valley, CA, 1982).